Germanium nanowires sheathed with an oxide layer

Y. F. Zhang, Y. H. Tang, N. Wang, C. S. Lee, I. Bello, and S. T. Lee*
Center of Super-Diamond & Advanced Films (COSDAF) and Department of Physics & Materials Science, City University of Hong Kong, Hong Kong, China

(Received 24 March 1999)

We report how the structural arrangement of germanium nanowires optimizes surface stability and enables the formation of very thin free-standing crystalline wires. Ge nanowires consisting of a crystalline Ge core and an amorphous GeO_2 sheath have been formed by laser ablation of a mixture of Ge and GeO_2. The crystalline Ge core lies in the axial [211] direction and is terminated by the {111} facets on the surface. The GeO_2 sheath saturates the surface bonds of the core, adapts to the core surface roughness, and prohibits the growth of the nanowire in the lateral direction. With such a core and sheath, the surface energy of the nanowire is reduced and the formation of very thin nanowires is thereby permitted. Phonon confinement in the Ge nanowires has been observed by Raman scattering.

Quasi-one-dimensional (1D) materials are a burgeoning and fascinating area of materials research that has significant technological implications.[1,2] Current interest focuses on several forms of quasi-1D materials, which include (i) shell structural nanotubes, such as carbon nanotubes, which can be formed from curved graphitic sheets with pentagonal and hexagonal networks of sp^2-bonded elemental carbons,[3,4] (ii) cast-in-tube nanowires, which are fabricated by filling hollow channel templates of porous anodic alumina and carbon tubes,[5,6] (iii) island-shaped nanowires, which are synthesized on a substrate surface using various techniques such as molecular beam epitaxy,[7] electron-beam lithogophy,[8] and scanning tunneling microscopy (STM) pattern writing,[9] and (iv) free-standing nanowires, which have been grown by laser ablation in vapor phase.[2,10–12] Nevertheless, the formation of free-standing nanowires is difficult due to the constraint of surface problems.

Surface energy is considered as a major factor that constrains the formation of nanoparticles.[13,14] For a cylindrical bare nanowire with a radius r and length L, the surface energy is given by

$$\sigma S(r) = 2\sigma V(r^{-1} + L^{-1}),$$

where σ is the surface energy or surface tension per unit area, $S(r)$ is the surface area of the nanowire, and V is the volume. For a certain volume of nanowire, there exists a reciprocal dependence between the surface energy and the radius of the nanowire. The thinner the bare nanowire, the higher the surface energy. The surface energies of shell structural nanotubes and cast-in-tube nanowires are low because there are no dangling bonds on their surface. The surface energy of the island-shaped nanowires should be also low because there is a large interface area between the island and the substrate. However, the surface energy of thin free-standing nanowires can be very high, especially for bare and sp^3-bonded covalent materials. The high surface energy may result in structural instability, and thus a lower limit may exist such that free-standing nanowires with diameters smaller than the threshold cannot form.

One possible way to facilitate the growth of free-standing nanowires is to reduce the surface free energy by saturating the surface bonds of nanowires with a suitable material that possesses low surface energy. Recently, we have reported a synthesis of Si nanowires via the laser ablation of a granulated mixture of Si and SiO_2.[15,16] The Si nanowires consist of a crystalline Si core and an amorphous SiO_2 sheath. Here, using a similar approach we report the successful synthesis of Ge nanowires via the laser ablation of a target made from a mixture of granulated Ge and GeO_2. The produced Ge nanowires consist of a crystalline Ge core and an amorphous GeO_2 sheath. Semiconductor Ge has long been an important material in high-speed microelectronics and infrared optical devices. Because of its small dimension, semiconductor Ge nanowires hold considerable promise in improving the indirect band-gap structure and optical properties of the material.

The apparatus utilized in the present work is similar to that used previously.[11,12,15,16] The production of Ge nanowires involves the laser ablation of a granulated mixture of Ge and GeO_2 in a quartz tube to generate a vapor phase of Ge subdioxide. The targets were composed of a mixture of Ge (purity 99.999%; particle size, 5 μm) and GeO_2 powder (obtained from the oxidation of high-purity Ge powder). The pulse energy of the laser was 450 mJ at a wavelength of 248 nm and a frequency of 10 Hz. The pulse duration was 34 ns. The argon flow rate through the quartz tube was 100 SCCM (cubic centimeters per minute at STP) at ~500 Torr. The temperature was 830 °C at the center of the quartz tube where the target was located. Approximately 15 cm downstream from the target, Ge deposits formed on the inner wall of the quartz tube and on the Si(111) substrate positioned near the tip of a copper cold finger, which was cooled by flowing water. Ge nanowires with diameters ranging from 16 to 500 nm formed in the areas where the substrate temperature fell within the narrow range of 690–705 °C. The nanowires grown at higher substrate temperature areas are relatively thinner. The yield of the nanowires is related to the amount of GeO_2 in the target, and the target composed of a molar percentage of 50% Ge and 50% GeO_2 yielded the maximum amount of Ge nanowires. The temperature and substrate position appeared to be very critical factors as well. Outside nanowire-forming areas, films and powders were deposited at the substrate areas where the temperature was higher than 705 °C and lower than 690 °C, respectively.

The Ge nanowires were taken directly from the substrate and held between two microscope specimen grids without

 ©2000 The American Physical Society

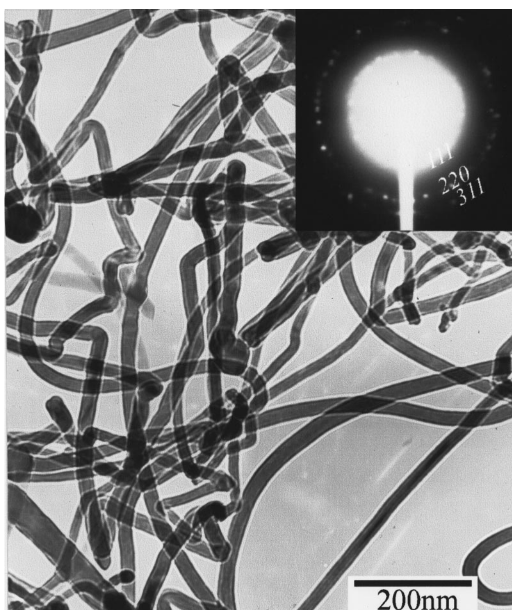

FIG. 1. A TEM image of Ge nanowires and a selected-area electron-diffraction pattern (inset).

any treatment for transmission electron microscopy (TEM) observation. A conventional transmission electron microscope (Philips CM20) was used at room temperature with an acceleration voltage of 200 kV. A TEM image of the Ge nanowires is shown in Fig. 1. The sample consists of nanowires with lengths up to a few tens of micrometers. Most of the wires are smoothly curved with some short straight sections, while some of them possess bends and kinks. The diameter of each nanowire is nearly the same throughout the length of the wire. The smallest diameter is measured to be ~12 nm with a core diameter of ~6 nm. Ge nanowires with diameters as large as ~190 nm are found at the place of a relatively lower temperature. The smooth and regular Ge nanowires were characterized by selected-area electron diffraction (SAED). Most of the electron-diffraction patterns show the discontinuous diffraction rings of crystalline Ge only, which consists of rather sharp spots. This indicates that the nanowires are well crystallized (Fig. 1 inset). The chemical composition was determined by micro-area *in situ* TEM energy-dispersive x-ray spectroscopy (EDX), and the result shows that the nanowires only contain Ge and oxygen. The profile lines running along the longitude of the nanowires is due to the Fresnel diffraction under the defocus condition in the TEM system.

Figure 2 shows the mass-thickness contrast TEM image of a thick Ge nanowire. The inset is the electron diffraction pattern with the incident electron beam being approximately parallel to the $[0\bar{1}1]$ direction. The nanowire consists of an amorphous GeO_2 sheath surrounding a crystalline Ge core with the axis in the [211] direction, with no relation to the crystalline direction of the Si substrate. The outside surface of the GeO_2 sheath is very smooth; however, the interface between the amorphous sheath and the crystalline core has an undulant contour, which can be seen more clearly in thicker nanowires. Many nanowires have been investigated and have all been found to adopt approximately the [211] direction. The profile between the core and the amorphous

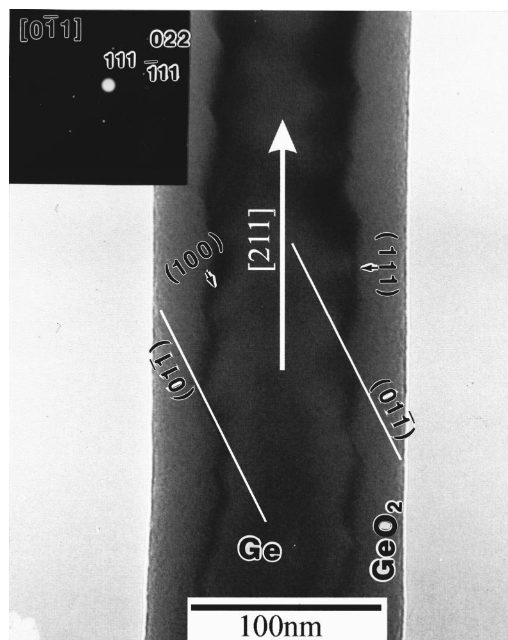

FIG. 2. A mass-thickness contrast TEM image of a thick Ge nanowire taken along the $[0\bar{1}1]$ zone axis and a selected-area electron diffraction pattern (inset).

Ge oxide sheath has a sawtooth contour. The edges of the teeth appear to be $(01\bar{1})$, (111), or slightly tilted (100) facets of the crystalline core. According to the geometry of the crystalline Ge lattice, the lattice plane (211) is not an atomically smooth plane. Significant atomic terraces exist on the (211) facets, and the ratio of the density of broken bonds in the (211) facet relative to the (111) is very high (1.41).[17] Therefore, [211] is a direction of high growth rate. The toothlike texture of the core surface is a naturally occurring configuration of the {011}, {100}, and {111} facets when the nanowire develops along the [211] direction. The amorphous Ge oxide sheath seems to have the ability to adapt to the toothlike texture of the core surface, and to saturate or passivate at least most of the core surface dangling bonds. This phenomenon has been generally identified by careful mass-thickness TEM observation. The contour of the sawtooth surface became dull as the diameter decreased; it can be clearly seen in thicker nanowires but is difficult to observe in thinner nanowires.

Figure 3 shows the morphology of the Ge nanowires at nucleation and budding stages. The sample was produced on a Si wafer at ~700 °C after a 2-min laser ablation. The nuclei and budding nanowires can be seen as nanosize hemispheres and short cylinders, respectively, on the substrate surface. The cylinders tilt at random angles with respect to the substrate surface. This morphology suggests that the deposition involves a much higher mass transport rate of ablated materials to the protruding tips than to the lateral side of the nanowires. No relations exist between the crystalline direction of the nanowire and the direction of the Si(111) substrate. TEM shows that the Ge nanowires at such a budding stage also consists of a Ge crystalline core and a Ge oxide surface layer (sheath). Since the budding wires could only be removed from the quartz tube after a long cooling-

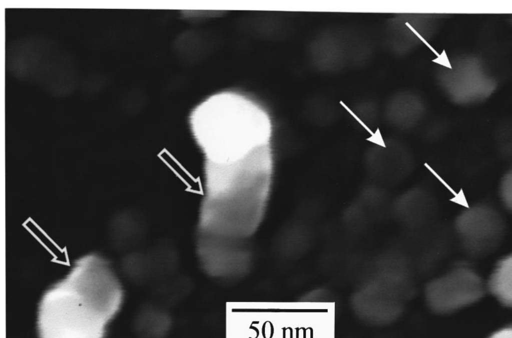

FIG. 3. A scanning electron microscopy image of the nuclei of Ge nanowires, which was taken from a Si(111) substrate after 2 min of growth. The typical hemisphere-shaped nuclei and cylinder-shaped budding of Ge nanowires are pointed by solid and hollow arrows, respectively.

down time, it has not been determined how spontaneously the phase segregation occurs during the nucleation of the Ge nanowires.

Chemical composition analysis showed that the atomic ratio of Ge to oxygen in the Ge nanowires was between 0.7 and 1.3. We propose the following formation mechanism of Ge nanowires. During the initial stage, substoichiometric germanium oxides ($GeO_x, x<2$) were formed at the nanowire tip. The GeO_x subsequently underwent reduction/oxidation or disproportionation to form Ge and GeO_2 under high-temperature annealing and subsequent phase separation into the Ge core and GeO_2 sheath with a concomitant decrease in the system free energy. This mechanism is supported by the observation that Ge nanocrystals form at 700–800 °C via phase separation in Ge-rich silicon oxide films.[18–20] Moreover, the formation of the smooth exterior surface of the GeO_2 sheath suggests that a viscous state of nanosize GeO_x exists at the tips of the nanowires during growth at ~700 °C, which is much lower than the temperature required for generating a viscous flow of GeO_2 ($\sim 850\,^{\circ}C$). Considering all these, the growth of Ge nanowires appears to follow the same oxide-assisted growth mechanism that we recently advocated for the synthesis of Si nanowires.[15,16] Four stages leading to the formation of Ge nanowires are proposed as follows.

(1) Laser ablation and chemical reaction: $Ge+GeO_2 \rightarrow GeO_x$ vapor.

(2) Deposition: GeO_xvapor$\rightarrow GeO_x$ deposits.

(3) Redox reaction: GeO_xdeposits$\rightarrow Ge+GeO_2$ mixture.

(4) Phase separation (incorporation of Ge atoms into the crystal lattice): $Ge+GeO_2$ mixture$\rightarrow$Ge core$+GeO_2$ sheath.

After a GeO_x hemisphere-shaped nucleus is formed on the substrate surface in stage (2), a Ge core will form in the interior and the crystalline lattice of the core via stages (3) and (4). The nanowire will continue to grow along the [211] direction following the deposition of the viscous GeO_x at the growth tip of the nanowire. The GeO_2 forms a sheath cladding the crystalline core, saturates the surface Ge dangling bonds of the core, and adapts to the surface roughness of the core. The smooth surface of the GeO_2 sheath reduces the surface free energy and inhibits the growth in the lateral direction.

It is difficult to determine the speed of formation of GeO_2.

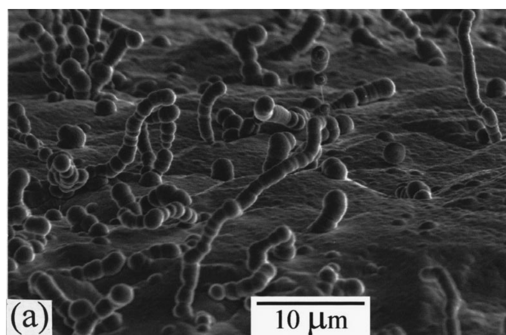

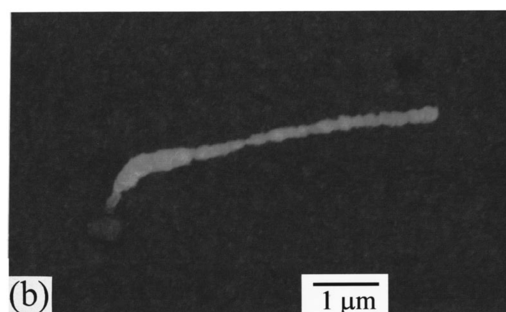

FIG. 4. The morphologies of the earthworm-shaped wires synthesized on a Si(111) substrate for 1 h by laser ablation of a mixture of 50% Ge and 50% SiO_2. The substrate temperature was (a) 700 °C and (b) 710 °C, respectively.

A few wirelike clumps of GeO_x, apparently due to incomplete phase segregation, were found deposited in the regions at temperature below 690 °C. Therefore, temperature is believed to be an important factor in inducing the phase segregation. From thermodynamic consideration, phase segregation and crystallization of the core of the nanowire are driven by decreasing system free energy.[21]

SiO_2 has a structure similar to GeO_2; however, the temperature needed to generate a viscous flow of substoichiometric silicon-germanium oxide should be higher than that of GeO_x. A test was done in conjunction with the above growth mechanism by substituting SiO_2 for GeO_2 in the target. Short and thick earthworm-shaped wires were grown on a ~700 °C Si substrate [Fig. 4(a)]. At the areas of the substrate surface where the temperature was higher (~710 °C), a few wires could also be observed, but they were relatively thinner [Fig. 4(b)]. Most wires have very coarse external surfaces, large diameters, and significantly low growth rates in length with respect to the deposition time. This may be explained by the possibility that the substoichiometric silicon-germanium oxide deposited at the growth tip was less viscous than the GeO_x. As a result, the phase separation in stage (4) slowed down significantly due to the substitution of SiO_2 for GeO_2. The larger diameter of the wires may be caused also in part by the increase of surface energy due to the coarse surface.

Free-standing Ge nanowires consisting of a crystalline core and an oxide sheath are suitable for creating relatively strong one-dimensional confinement effects on electrons, holes, and phonons because they can be gathered together in high density as piles or bundles while each individual wire is electrically and optically isolated. Compared to Si, Ge has smaller electron and hole effective masses and a lower dielectric constant, so Ge nanowires may be expected to exhibit more pronounced quantum confinement characteristics

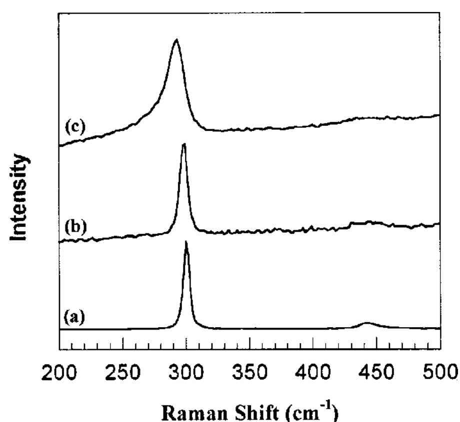

FIG. 5. Room-temperature Raman spectra for (a) a single-crystalline Ge wafer, and Ge nanowires with nominal diameters of (b) 36–83 nm and (c) 12–28 nm [corresponding core diameters: (b) 20–51 nm, (c) 6–17 nm].

than that of the Si nanowire at a similar diameter. Raman spectroscopy is a suitable tool for investigating the phonon confinement effect of nanomaterials.[21] The peak-position shift, broadening, and asymmetry of the Raman bands have been observed in Ge nanocrystals.[22] We performed Raman scattering measurements of Ge nanowires at room temperature using a micro-Raman system (Renishaw 2000) with 1 cm^{-1} resolution and 0.4 cm^{-1} reproducibility. The excitation source was a 514.5-nm argon-ion laser line with a spot size of 10 μm in diameter and a power of 2 mW. The Raman spectrum was recorded on a sample spot that was predominantly flat and uniform in content. The Raman spectra of two Ge nanowire samples with different nominal diameters (12–28 and 36–83 nm) and a single-crystalline Ge(c-Ge) wafer were recorded. The first-order Raman peak of c-Ge at 298.5 cm^{-1} is symmetrical with a full width at half maximum (FWHM) of 7 cm^{-1} [Fig. 5(a)]. Raman scattering from the Ge nanowire sample with diameters of 36–83 nm (corresponding core diameters of ~20–51 nm) shows a peak at 298.5 cm^{-1} that is slightly broadened (a FWHM of 10 cm^{-1}) and asymmetric [Fig. 5(b)]. Figure 5(c) is a typical Raman spectrum of Ge nanowires with diameters ranging from 12 to 28 nm (corresponding core diameters ~6–17 nm). The Raman peak at 293 cm^{-1} is asymmetric with a FWHM of 21 cm^{-1} and has an extended tail at low frequencies.

Because no stress-induced lattice parameter change of the Ge core has been detected, the profile and shape of the Raman peak may be mainly attributed to the quantum confinement of optical phonons in the Ge nanowires. The small physical dimension of the scattering crystalline nanowires leads to a downshift and broadening of the first-order Raman line through a relaxation of the $q=0$ selection rule. Because the nanowires are long and thin crystals, there is a momentum $q=0$ along their axis direction. Hence, the zone-center phonons allow for the Raman scattering to occur at 298.5 cm^{-1}. However, in the direction perpendicular to the axis of nanowires, the crystal size d is small with the corresponding momentum $q=\pm 2\pi/d$. Therefore, nonzero q phonon dispersion, which includes the optical phonons (LO and TO) of Ge, may participate in Raman scattering and lead to both a peak broadening and an extension of the Raman peak towards low frequencies. Raman scattering is very sensitive to the lattice microstructure and crystal symmetry of microcrystalline materials. When the core diameter of a Ge nanowire is small, the Raman peak width increases and becomes more asymmetric with an extended tail at low frequencies. Because the diameters of Ge nanowires and thus the finite crystal size d have a wide distribution, an extended tail at low frequencies thus arises in the Raman spectrum.

In conclusion, Ge nanowires have been synthesized by an oxide-assisted growth technique in a laser ablation system. The Ge nanowire consisted of an amorphous GeO_2 sheath and a single-crystalline Ge core with a [211] axis. Ge oxide was needed in the target for the formation of Ge nanowires. The proposed growth mechanism of Ge nanowires is concerned mainly with the deposition of substoichiometric germanium oxide and subsequent phase separation into Ge and GeO_2. The GeO_2 sheath played an important role in the formation of Ge nanowires through reducing the surface energy by saturating the surface bonds and terminating the growth in the lateral direction with a smooth GeO_2 surface. The phonon confinement effect has been revealed by Raman scattering in Ge nanowires with core diameters of 6–17 nm.

The authors wish to thank Professor F. H. Li for useful discussions. This work was supported in part by the Research Grants Council of Hong Kong (Project No. 9040459) and the Strategic Research Grant of the City University of Hong Kong.

*Author to whom all correspondence should be addressed. FAX: (852) 2784-4696. Electronic address: apannale@cityu.edu.hk

[1] A. P. Alivisatos, Science **271**, 933 (1996).
[2] O. Gulseren *et al.*, Phys. Rev. Lett. **80**, 3775 (1998).
[3] S. Iijima, Nature (London) **354**, 56 (1991).
[4] M. S. Dresselhaus *et al.*, *Science of Fullerenes and Carbon Nanotubes* (Academic, San Diego, 1996).
[5] A. N. Govyadinov and S. A. Zakhvitcevich, J. Vac. Sci. Technol. B **16**, 1222 (1998).
[6] A. A. Setlur *et al.*, Appl. Phys. Lett. **69**, 345 (1996).
[7] H. Omi and T. Ogino, Appl. Phys. Lett. **71**, 2163 (1997).
[8] H. Namatsu *et al.*, J. Vac. Sci. Technol. B **13**, 1473 (1995).
[9] N. Kramer *et al.*, Appl. Phys. Lett. **66**, 1325 (1995).
[10] A. M. Morales and C. M. Lieber, Science **279**, 208 (1998).
[11] Y. F. Zhang *et al.*, Appl. Phys. Lett. **72**, 1835 (1998).
[12] N. Wang, Y. H. Tang, Y. F. Zhang, C. S. Lee, and S. T. Lee, Chem. Phys. Lett. **283**, 368 (1998).
[13] M. S. El-Shall and A. S. Edelstein, in *Nanomaterials: Synthesis, Properties and Applications*, edited by A. S. Edelstein and R. C. C. Cammarata (Institute of Physics, Bristol, 1996), p. 13.
[14] N. Fukuta and R. H. Wagner, *Nucleation and Atmospheric Aerosols* (Deepak, Hampton, VA, 1992).
[15] N. Wang *et al.*, Phys. Rev. B **58**, R16 024 (1998).
[16] Y. F. Zhang *et al.*, J. Cryst. Growth **197**, 136 (1999).
[17] R. J. Jaccodine, J. Electrochem. Soc. **110**, 524 (1963).
[18] A. K. Dutta, Appl. Phys. Lett. **68**, 1189 (1996).
[19] M. Fuji *et al.*, Jpn. J. Appl. Phys., Part 1 **30**, 687 (1991).
[20] Y. Maeda *et al.*, Appl. Phys. Lett. **59**, 3168 (1991).
[21] F. X. Liu *et al.*, Phys. Rev. B **55**, 8847 (1997).
[22] T. Kanata *et al.*, J. Appl. Phys. **61**, 969 (1987).